CHEMICAL ENGINEERING TRANSACTIONS
VOL. 101, 2023
A publication of AIDIC
The Italian Association of Chemical Engineering
Online at www.cetjournal.it
Guest Editors: Paolo Ciambelli, Luca Di Palma

ISBN 979-12-81206-00-7; **ISSN** 2283-9216
DOI: 10.3303/CET23101038

Investigation of Oxygen Vacancies in Sputtered GDC Thin Films Probed via *Operando* XAS

Nunzia Coppola[a*], Hafiz Sami Ur Rehman[b], Giovanni Carapella[c], Luca Braglia[d], Dario Montinaro[e], Piero Torelli[d], Luigi Maritato[a], Carmela Aruta[f], Alice Galdi[a]

[a] Dipartimento di Ingegneria Industriale-DIIN, Università Degli Studi di Salerno and CNR-SPIN, 84084 Fisciano (SA), Italy;
[b] Dipartimento di Ingegneria Industriale-DIIN, Università Degli Studi di Salerno, 84084 Fisciano (SA), Italy;
[c] Dipartimento di Fisica "E.R. Caianiello", Università Degli Studi di Salerno, and CNR-SPIN,84084 Fisciano (SA), Italy;
[d] National Research Council CNR-IOM, TASC National Laboratory, I-34149 Trieste, Italy
[e] SolydEra S.p.A., Viale Trento 117, 38017 Mezzolombardo (TN), Italy
[f] National Research Council CNR-SPIN, Area della Ricerca di Tor Vergata, 00133 Rome, Italy
ncoppola@unisa.it

In previous works, we reported that Solid Oxide Fuel Cells (SOFCs), having a room-temperature sputtered and then annealed GDC thin film as the cathode/electrolyte barrier layer, had showed a huge increase of the output current (up to +78%) and a decrease of the ohmic resistance (up to -42%) as compared to fully screen-printed industrial SOFCs. We correlated the performance improvement to grain size in the GDC layer as a function of annealing temperature. However, no information on the density and activity of oxygen vacancies in the thin film to correlate with functionality could be extrapolated in these studies.
Element and valence sensitive probes such as X-Ray Photoelectron Spectroscopy (XPS) and X-Ray Absorption Spectroscopy (XAS) enable atomic level characterization of nanostructured granular GDC layers deposited on polycrystalline anode/electrolyte bilayer substrates and the interplay between morphology and stoichiometry in determining the Ce^{3+}/Ce^{4+} ratio, which in turns regulates their ionic and electronic conductivity.
Here we show the results obtained on three room-temperature RF-sputtered GDC thin films, annealed with the same annealing ramp but at different plateaux temperatures, making use of XPS measurements to study the unreacted surface and the *operando* XAS to monitor the changes in Ce^{3+}/Ce^{4+} ratio in different reactive atmospheres (i.e. neutral, oxidizing and reducing). The latter were carried out using the ambient pressure cell available at APE-HE beamline (Elettra synchrotron in Trieste, Italy). Our measurements allowed to determine the role of the annealing parameters in the number of available oxygen vacancies available in the oxygen reduction reaction (ORR), highlighting the different modifications induced in the investigated samples by the annealing process.

1. Introduction

Partially substituted trivalent rare earth cerium oxides attracted interest in the past years due to their versatility and catalytic properties, which make them well qualified for a wide range of applications(Kuhn et al. 2013; Ackermann et al. 2015; Yang et al. 2016).
In particular, it is now established that the oxygen evolution reaction (Kumar et al. 2013; Siebenhofer et al. 2022) used to generate electricity in Solid Oxide Fuel Cells (SOFCs) depends on the ionic transport through the electrolyte and the so-called barrier layer which is usually a gadolinium doped ceria (GDC) layer. Furthermore, it is well known that, in GDC barrier layer of SOFC, the ion conductivity is related to the hopping of oxygen ions through the oxygen vacancy sites in the lattice and that the mechanism of oxygen vacancy formation consists in the Ce valence change (from Ce^{4+} to Ce^{3+}) induced by Gd doping (Yang et al. 2017).
Thus, once the percentage of Gd doping is fixed, the ionic conductivity of the GDC layer can vary depending on the specific structure, granularity, defect incorporation and density of oxygen vacancies induced in the film lattice.

Paper Received: 5 February 2023; Revised: 16 March 2023; Accepted: 28 May 2023
Please cite this article as: Coppola N., Ur Rehman H.S., Carapella G., Braglia L., Montinaro D., Torelli P., Maritato L., Aruta C., Galdi A., 2023, Investigation of Oxygen Vacancies in Sputtered GDC Thin Films Probed via Operando XAS, Chemical Engineering Transactions, 101, 223-228 DOI:10.3303/CET23101038

In previous work (Coppola et al. 2020), in the case of room-temperature sputtered GDC barrier layers, we demonstrated that, by reducing the mean GDC grain size by decreasing the post-growth annealing temperature, the complete SOFC shows both a very large increase in the output current and a simultaneous decrease in the ohmic resistance of the SOFC. However, in these studies no information was extrapolated on the density and activity of oxygen vacancies in the thin film. Since the aforementioned GDC layer fabrication process (Coppola et al. 2020; Coppola et al. 2018b) has proved feasible also in the case of industrial scale SOFC (Coppola et al. 2021, Coppola et al.2023), it is interesting and noteworthy to achieve a deeper understanding of microscopic differences among sputtered GDC thin film barrier layer as a function of post-growth annealing treatment in view of further optimization of industrial scale SOFCs.
Here we show the results obtained on three RF-sputtered GDC thin films at room-temperature , annealed with the same annealing ramp but at different plateau temperatures, using two different spectroscopic techniques, namely X-Ray Photoemission Spectroscopy (XPS) measurements to study the unreacted surface, and *operando* X-Ray Absorption Spectroscopy (XAS) to investigate the changes in Ce^{3+}/Ce^{4+} ratio in neutral and reducing atmosphere. XAS measurements were carried out using the ambient pressure cell available at APE-HE beamline (Elettra synchrotron, Trieste, Italy).

2. Materials and Methods

2.1 Thin Film Deposition

Three $Gd_{0.1}Ce_{0.9}O_{1.95-\delta}$ (GDC) thin films of 300 nm thickness were sputtered at room-temperature using an RF-sputtering equipped with a 15 cm diameter 99.999% purity target (Testbourne). The deposition parameters are reported in (Coppola et al. 2018a; Coppola et al. 2018b). The substrate used consists in NiO/YSZ polycrystalline bilayers (SolydEra S.p.A, Mezzolombardo (Italy)) cut into slivers of 5x5 mm^2.
Two of the as-grown samples were thermally treated using the annealing ramps described in (Coppola et al. 2020).
All samples are RF-sputtered at room-temperature and have the same composition, but the only difference among them relies in the post-growth annealing ramp plateau temperature:

- Sample GDC800 is annealed with a 800°C plateau temperature
- Sample GDC1000 is annealed with a 1000°C plateau temperature,
- Sample GDC-As- grown

2.2 X-ray Diffraction (XRD)

The crystal structure of the deposited thin films was investigated both before and after annealing using a D2-Phaser diffractometer equipped with a Cu-Kα radiation source characterized by a wavelength λ= 1.541 Å. All the spectra were acquired setting 2θ=0.01° as angular resolution and 0.4s as acquisition time.

2.3 X-Ray Photoemission Spectroscopy (XPS)

The sample surface was analyzed using the XPS core level spectra acquired using a TX400 X-ray photoemission spectroscope equipped with an Al source cathode (with K_α = 1486,7 eV) available at the Elettra Synchrotron as an offline facility of the APE-HE beamline. The measurements were carried out at a pressure of 10^{-9} bar and a pass energy of 50 eV. The analyzer mean radius is 200mm. The X-rays hit the sample at 45° with respect to the source. The survey scans were acquired with a channel width of 2.3 mm while a channel width of 1.1 mm was selected for the element-specific scans. The energy calibration of all spectra was performed using the Au 4f reference spectra acquired after each sampling run.

2.4 *Operando* X-Ray Absorption Spectroscopy (XAS)

XAS spectra were acquired in *operando* using the ambient pressure cell present at the APE-HE beamline of the Elettra Synchrotron. A detailed description of the cell and the silicon nitride membrane used during the experiment can be found in (Castán-Guerrero et al. 2018). a two-contact measurement (one contact on the membrane, the other one on the sample) allowed to obtain the XAS total electron yield (TEY) signal. The spectra were acquired in neutral (1 bar He gas) and reducing (1 bar H_2 gas) atmospheres at temperatures ranging from room temperature up to about 300 °C.

3. Results

The GDC800, GDC1000 and GDC-As-grown samples were preliminary studied using XRD measurements both before and after the annealing treatment. The obtained results are shown in Figure 1.

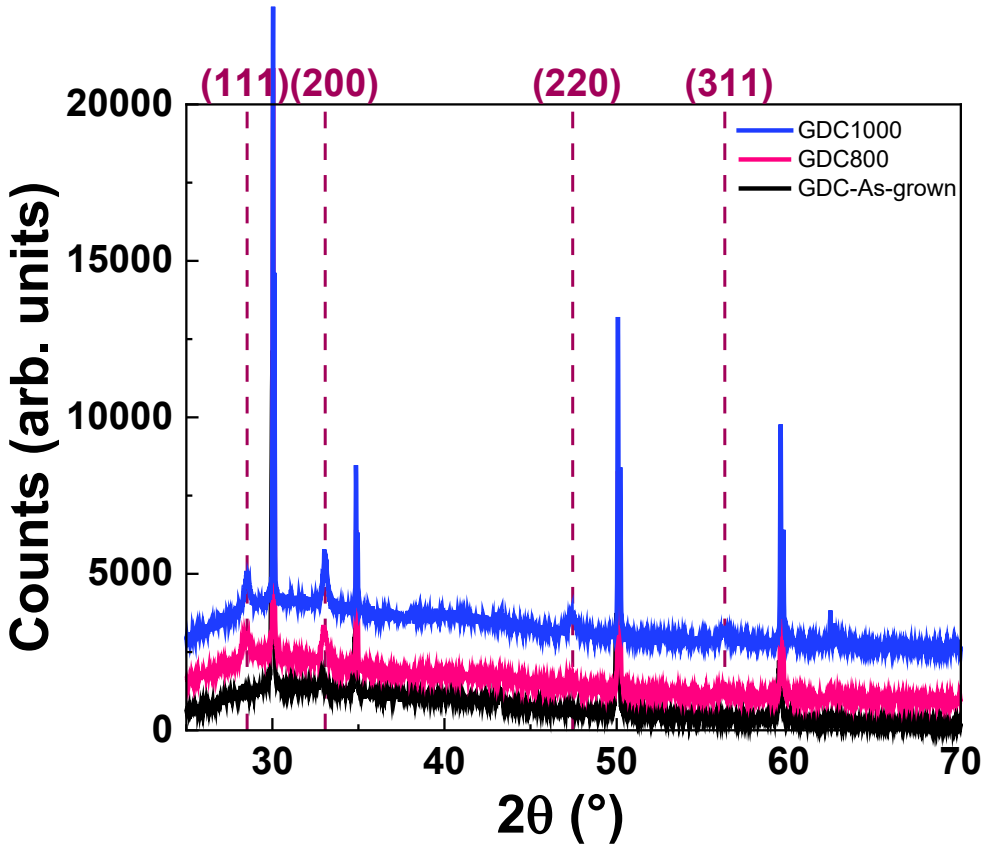

Figure 1 XRD spectra of the analysed samples: sample GDC-As-grown (black line), sample GDC800 (pink line) and sample GDC1000 (blue line). Dashed burgundy lines are in correspondence of the angular positions of the bulk GDC reflections in terms of Miller indices found in literature(Cheng et al. 2002).

By comparing the XRD spectra it is evident that the as-grown sample shows GDC peaks at lower angular positions than the values reported in literature and thus the evaluated c-axis parameter is higher than the literature values, being ≈ 5.45 Å. However, both annealed samples show all the visible peaks at bulk angular positions corresponding to the expected calculated value of the c-axis ≈ 5.41 Å. Therefore, no structural differences induced by the different plateau temperatures of the annealing ramp are evident from the XRD spectra. Moreover, it is not possible to extrapolate a difference in the oxygen content induced in the GDC lattice by the annealing ramp in GDC800 and GDC1000 samples. On the contrary, the comparison among the XPS spectra (Figure 2) of the three samples highlights the actual differences induced by the post-growth treatment. In particular, by looking at Figures 2b and 2c it can be noticed that the three samples are characterized by different relative intensities of the features associated to different valence states (in case of Ce) and different types of surface oxygen (namely lattice oxygen, vacancies and OH^- species) (Yang et al. 2016).
The above results allow us to conclude that, even if no structural difference is highlighted by XRD, on the contrary, the GDC800 and GDC1000 samples present different amounts of Ce^{3+} and Ce^{4+} (and therefore a different amount of oxygen vacancies in the lattice) and this result is accordingly accompanied by differences in the O 1s core level spectra.
The second part of the experiment consisted in *operando* XAS spectra acquisition performed on the same samples previously mentioned. The results obtained at Ce $M_{4,5}$ absorption edge for the GDC800 and GDC1000 samples are summarized in Figure 3.

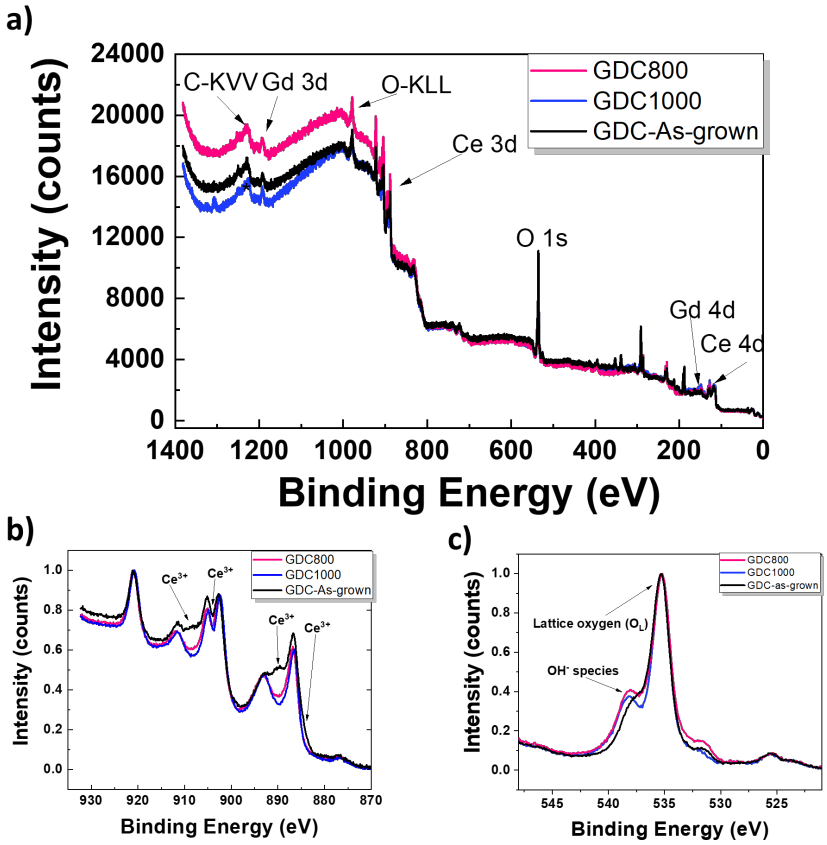

Figure 2 XPS spectra of samples GDC800 (pink line), GDC1000 (blue line), GDC-As-grown (black line). In a) the survey scan performed on the whole energy range is displayed while in b) and c) details of the Ce $3d_{3/2}$ and $3d_{5/2}$ and O 1s core levels are shown respectively.

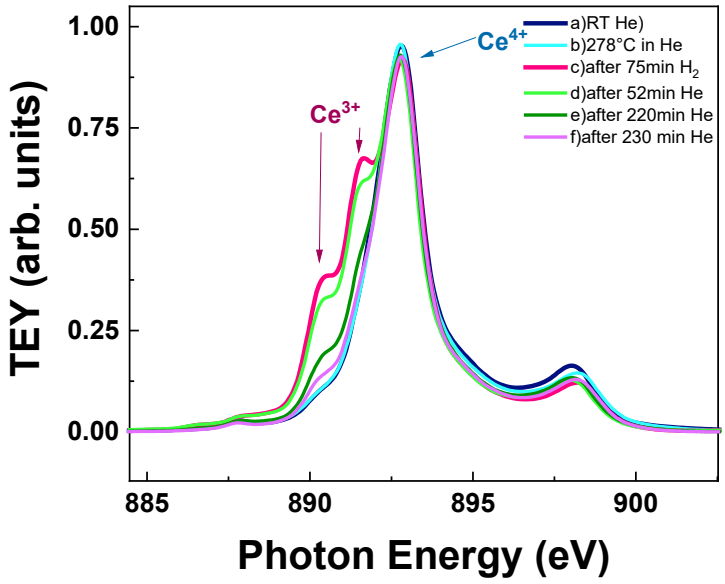

Figure 3 In operando XAS evolution of the Ce M_5 absorption edge of the GDC800 sample in He/H_2 atmosphere over exposure time and at different temperatures. Red arrows indicate the peak related to the Ce^{3+} formation, while the blue arrow indicates the main peak associated to the oxidized Ce (Ce^{4+}).

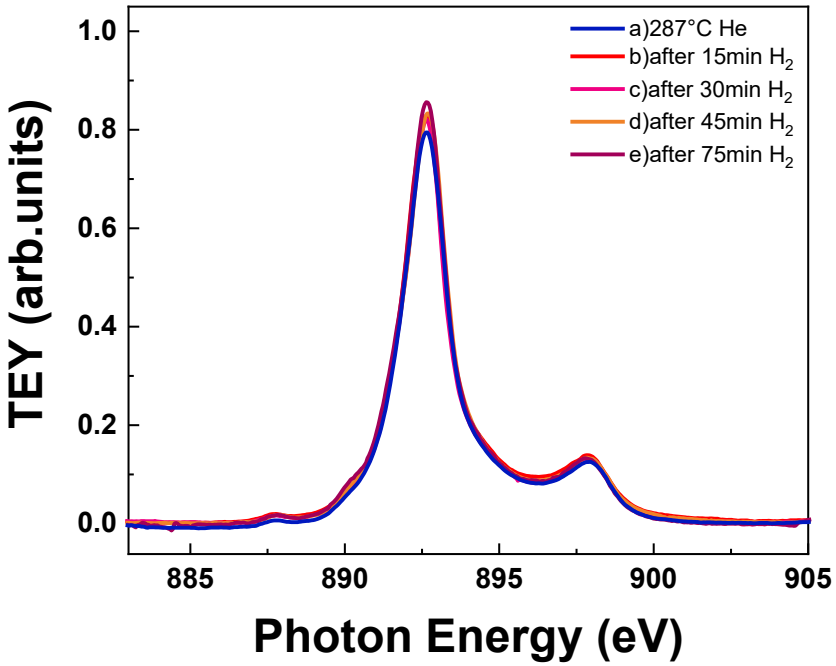

Figure 4 In operando XAS evolution of the Ce M_5 absorption edge of the of the GDC1000 sample in He/H_2 atmosphere over exposure time.

The XAS spectra shown in Figures 3 and 4 allow to verify the different reactivity of samples annealed with different plateau temperatures and characterized by different initial Ce^{3+}/Ce^{4+} ratios and therefore a different amount of oxygen vacancies. Indeed, while GDC800 sample is characterized by an evident evolution of the features associated to Ce^{3+} and Ce^{4+} as a function of the atmosphere and temperature at which it is exposed during the XAS measurement, on the contrary, the sample annealed at higher plateau temperature is characterized by a very poor evolution of the Ce M_5 XAS spectra. This last observation indicates a better oxygen ionic conductivity and surface exchange rate of GDC800 sample compared to GDC1000, providing a first hint on the nature of the behavior of samples studied in (Coppola et al. 2020).

4. Conclusions

Sputtered GDC thin films deposited on industrial substrates and annealed at different temperatures were structurally and spectroscopically characterized by XRD, XPS and *operando* XAS. XRD showed that the analyzed samples are characterized by the same lattice parameter, thus not allowing to distinguish any differences in the oxygen content induced by the annealing temperature.
Conversely, XPS and XAS measurements highlight the presence of dissimilarities in the thermally treated thin films with different annealing ramps, mainly in terms of oxygen content. In fact, XPS performed on the surface of unreacted samples allows to attribute a higher amount of Ce^{3+}, and thus a higher number of oxygen vacancies, to the GDC800 sample. On the contrary, the GDC1000 sample is characterized by a greater quantity of Ce^{4+}.
The variation of the Ce^{3+}/Ce^{4+} ratio that characterizes the GDC thin films studied here is reflected in the evolution of the absorption spectra at the Ce M_5 edge probed via the *operando* XAS. The sample annealed at lower temperature, i.e. GDC800, is characterized by a higher ionic mobility, being characterized by the highest changes in the shape of the Ce M_5 edge in both oxidizing and reducing atmospheres. These results are in agreement with the results presented in (Coppola et al. 2018b; Coppola et al. 2020) and may provide hints on the annealing-induced microscopic changes of GDC thin films that positively contribute to the final performance of SOFCs.

References

Ackermann S, Sauvin L, Castiglioni R, Rupp JLM, Scheffe JR, Steinfeld A. Kinetics of CO2 Reduction over Nonstoichiometric Ceria. J Phys Chem C. 2015;119(29):16452–61.

Castán-Guerrero C, Krizmancic D, Bonanni V, Edla R, Deluisa A, Salvador F, et al. A reaction cell for ambient pressure soft x-ray absorption spectroscopy. Rev Sci Instrum [Internet]. 2018;89(5). Available from: http://dx.doi.org/10.1063/1.5019333

Cheng J gui, Zha S wu, Huang J, Liu X qin, Meng G yao. Powder Prepared By the Gel-Casting Process. 2002;78(2003):791–5.

Coppola N, Carapella G, Sacco C, Orgiani P, Galdi A, Polverino P, et al. Investigation of Interface Diffusion in Sputter Deposited Gd0.1Ce0.9O1.95 Thin Buffer Layers on Y-Stabilized Zirconia Crystalline Substrates for Solid Oxide Cells Applications. J Mater Sci Eng. 2018a;07(05).

Coppola N, Polverino P, Carapella G, Ciancio R, Rajak P, Montinaro D, et al. Large Area Deposition by Radio Frequency Sputtering of Gd0.1Ce0.9O1.95 buffer layers in Solid Oxide Fuel Cells: Structural, Morphological and Electrochemical Investigation. Materials (Basel). 2021;14:5826.

Coppola N, Ur Rehman HS, Carapella G, Polverino P, Montinaro D et al., Large area solid oxide fuel cells with room temperature sputtered barrier layers: Role of the layer thickness and uniformity in the enhancement of the electrochemical performances and durability. Int J Hydrogen Energy 2023, https://doi.org/10.1016/j.ijhydene.2023.04.170

Coppola N, Polverino P, Carapella G, Sacco C, Galdi A, Montinaro D, et al. Optimization of the electrical performances in Solid Oxide Fuel Cells with room temperature sputter deposited Gd0.1ce0.9o1.95 buffer layers by controlling their granularity via the in-air annealing step. Int J Hydrogen Energy [Internet]. 2020;45(23):12997–3008. Available from: https://doi.org/10.1016/j.ijhydene.2020.02.187

Coppola N, Polverino P, Carapella G, Sacco C, Galdi A, Ubaldini A, et al. Structural and electrical characterization of sputter-deposited Gd0.1Ce0.9O2−δ thin buffer layers at the Y-stabilized zirconia electrolyte interface for IT-solid oxide cells. Catalysts. 2018b;8(12).

Kuhn M, Bishop SR, Rupp JLM, Tuller HL. Structural characterization and oxygen nonstoichiometry of ceria-zirconia (Ce1-xZrxO2-δ) solid solutions. Acta Mater. 2013;61(11):4277–88.

Kumar A, Leonard D, Jesse S, Ciucci F, Eliseev EA, Morozovska AN, et al. Spatially resolved mapping of oxygen reduction/evolution reaction on solid-oxide fuel cell cathodes with sub-10 nm resolution. ACS Nano. 2013;7(5):3808–14.

Siebenhofer M, Riedl C, Schmid A, Limbeck A, Opitz AK, Fleig J, et al. Investigating oxygen reduction pathways on pristine SOFC cathode surfaces by: In situ PLD impedance spectroscopy. J Mater Chem A. 2022;10(5):2305–19.

Yang N, Orgiani P, Di Bartolomeo E, Foglietti V, Torelli P, Ievlev A V., et al. Effects of Dopant Ionic Radius on Cerium Reduction in Epitaxial Cerium Oxide Thin Films. J Phys Chem C. 2017;121(16):8841–9.

Yang N, Shi Y, Schweiger S, Strelcov E, Belianinov A, Foglietti V, et al. Role of Associated Defects in Oxygen Ion Conduction and Surface Exchange Reaction for Epitaxial Samaria-Doped Ceria Thin Films as Catalytic Coatings. ACS Appl Mater Interfaces. 2016;8(23):14613–21.